

## MIT Open Access Articles

*Earthquake Depth Phase Extraction With P  
Wave Autocorrelation Provides Insight Into  
Mechanisms of Intermediate#Depth Earthquakes*

The MIT Faculty has made this article openly available. **Please share**  
how this access benefits you. Your story matters.

**Citation:** Fang, Hongjian and Hilst, Robert D. 2019. "Earthquake Depth Phase Extraction With P Wave Autocorrelation Provides Insight Into Mechanisms of Intermediate#Depth Earthquakes." Geophysical Research Letters, 46 (24).

**As Published:** <http://dx.doi.org/10.1029/2019gl085062>

**Publisher:** American Geophysical Union (AGU)

**Persistent URL:** <https://hdl.handle.net/1721.1/140983>

**Version:** Author's final manuscript: final author's manuscript post peer review, without publisher's formatting or copy editing

**Terms of use:** Creative Commons Attribution-Noncommercial-Share Alike



# Earthquake depth phase extraction with P-wave auto-correlation provides insight into mechanisms of intermediate-depth earthquakes

Hongjian Fang<sup>1</sup>, Robert D. van der Hilst<sup>1</sup>

<sup>1</sup>Department of Earth, Atmospheric and Planetary Sciences, Massachusetts Institute of Technology, 77 Mass Ave,  
Cambridge, MA 02139, USA

## Key Points:

- Autocorrelating teleseismic P wave improves focal-depth estimates for intermediate-depth earthquakes, with moment magnitude down to 4.0
- Slab age correlates with the width of the double seismic zone observed in relocated catalogs for the Japan and Chile subduction zones
- The dry lower layers in the double seismic zones call for other mechanisms to interpret the intermediate-depth earthquakes rather than dehydration

This is the author manuscript accepted for publication and has undergone full peer review but has not been through the copyediting, typesetting, pagination and proofreading process, which may lead to differences between this version and the [Version of Record](#). Please cite this article as doi: [10.1029/2019GL085062](https://doi.org/10.1029/2019GL085062)

Corresponding author: Hongjian Fang, [hfang@mit.edu](mailto:hfang@mit.edu)

## Abstract

Constraining the mechanism of earthquakes in subduction zones requires adequate estimates of source location and near-source elastic properties. In this study, we propose a P-wave auto-correlation based method to extract depth phase energy from teleseismic earthquakes with moment magnitude down to 4.0. We apply the method to improve location estimates of intermediate-depth earthquakes in the Japan and northern Chile subduction zones, which represent so-called cold and warm slabs, respectively, and which are both marked by double seismic zones. A positive correlation of slab age and double-seismic-zone width validates a thermally-controlled model of slab morphology. The negative to normal differential times (and, thus, low or normal  $V_p/V_s$ ) of the deep parts of the double seismic zones suggest that the intermediate-depth earthquakes considered here are not due to dehydration.

## Plain Language Summary

Earthquake depth, which can be obtained by using depth phases, is critical for hazard mitigation and a better understanding of their mechanisms. Most techniques that use depth phases with teleseismic data require large events, even when array-based techniques are used, which limits comprehensive studies of subduction zone seismicity. Here we propose a new auto-correlation based method to extract depth phase energy from teleseismic data generated by earthquakes with magnitudes as small as  $M_w 4.0$ . The application to Japan and northern Chile validates the robustness of the method, and the more precise delineation of the double seismic zones reveals a positive correlation between their widths and the age of the slab when it approaches the trench. Moreover, we find the differential times of sP and pP energy, which are sensitive to the average  $V_p/V_s$  between the events and the surface, are different between the upper and the lower layer in the double seismic zone, with the lower layer mostly showing negative to normal values and thus low or normal  $V_p/V_s$ . This indicates a lack of water in the lower layer and suggests that other mechanisms are needed to interpret intermediate earthquakes rather than dehydration.

## 1 Introduction

Since their discovery in the 1920s [Turner, 1922; Wadati, 1928], the mechanism of deep earthquakes remained enigmatic, in part, due to the absence of experimental evidence for rock rupture at high temperature and pressure. Transformational faulting can

explain the peak of seismicity around 550 km and the cessation at 700 km [Green, 1995; Houston, 2007] and has been proposed as the likely cause of most deep-focus earthquakes (>300 km). For intermediate-depth (50 - 300 km) earthquakes, two main mechanisms have been proposed based on experimental, seismological, and geological evidence [Houston, 2007]: dehydration embrittlement and thermal shear instability.

Dehydration embrittlement invokes the increase of pore pressure caused by metamorphic reactions [Hacker *et al.*, 2003; Houston, 2007], which decreases effective friction and permits rocks to rupture. Many geophysical observations are consistent with this mechanism, such as pervasive normal faults in the outer rise of trenches that allow water to infiltrate before subduction [Grevemeyer *et al.*, 2007; Ranero *et al.*, 2003, 2005], the positive correlation of seismicity rate and fault density on incoming plates [Boneh *et al.*, 2019; Shillington *et al.*, 2015], thermal-controlled metamorphic dehydration from thermal-chemical modeling [Chen *et al.*, 2019; Kita *et al.*, 2006; Wei *et al.*, 2017], and highly-conductive anomalies above intermediate-depth earthquakes imaged using magnetotellurics [Vargas *et al.*, 2019] or very low wavespeed anomalies from guided waves [Shiina *et al.*, 2013, 2017]. Laboratory experiments also show evidence for dehydration-related brittle deformation [Dobson, 2002; Jung *et al.*, 2004, 2009; Okazaki and Hirth, 2016], although cases exist where only slow slip events are observed [Chernak and Hirth, 2011].

An alternative mechanism has been proposed in which the thermal shear instability occurs due to the positive feedback between temperature-dependent viscosity and slip in a localized shear zone [John *et al.*, 2009; Kelemen and Hirth, 2007]. Kelemen and Hirth [2007] simulated quasi-periodic instabilities inside localized fine-grained shear zones in their numerical models, with a temperature of 600 – 800°C and strain rate of  $10^{-15}/s$  to  $10^{-12}/s$ , which correspond well with the conditions of intermediate-depth earthquakes. This is consistent, for instance, with the high temperature during fault failures inferred from the high stress drop and low radiation efficiency of the intermediate-depth earthquakes of the Bucaramanga Nest [Prieto *et al.*, 2013]. Besides the numerical and seismic evidence, geological observations of pseudotachylites in subduction zones that are formed by melting during earthquake ruptures also indicate evaluated temperature above the melting points [Obata and Karato, 1995; Ueda *et al.*, 2008; Deseta *et al.*, 2014] and are, thus, consistent with a thermal shear instability mechanism.

Debate continues, however, over which of these mechanisms is active, or predominant, in the intermediate depth range [e.g. *Peacock, 2001; Reynard et al., 2010*]. To understand the mechanisms of intermediate-depth earthquakes better, accurate source locations and knowledge about elastic properties around the source region are of great importance. In this paper, we propose a new method to extract energy associated with the arrival of seismic depth phases (here, pP and sP) in order to determine earthquake depth more accurately. We also calculate the differential arrival time between sP and pP to characterize the Poisson's ratio around the source region to constrain the effect of dehydration. Similar to *Tibuleac [2014]* and *Audet and Ma [2018]*, our method relies on auto-correlation to align the P wave, but we adopt a spectral broadening scheme to normalize the contribution of different frequency contents, which turns out to have a critical influence on the final results. Since the arrival time of depth phases changes more slowly with respect to epicentral distance than to depth, we can stack the auto-correlograms coherently with a simple move-out correction, thus greatly increasing the signal-to-noise ratio of depth phase energy by using the abundant distribution of broad-band seismic stations at teleseismic distances (that is,  $\Delta > 30^\circ$ ). This allows us to detect and extract depth phase energy from earthquakes that are smaller (down to  $M_w 4.0$ ) than those considered in other array-based studies, which usually require large earthquakes ( $M_w > 5.0$ ) to get a sufficient signal to noise ratio [*Craig, 2019; Florez and Prieto, 2017*]. The proposed method, as well as other auto-correlation based techniques, could be seen as time-domain equivalents of the 'Cepstral' method [e.g. *Kemerait and Sutton, 1982; Bonner et al., 2002*], which has been used to detected echoes, such as pP and sP, after the first P-wave arrival. Our method does not require a large signal to noise ratio, however, which makes it suitable for application to teleseismic data and, especially, for relatively small events ( $M_w < 5.0$ ).

In the following sections, we will first introduce the data processing and then illustrate and validate our method with a  $M_w 4.5$  intermediate earthquake in northern Chile. We then apply the method to intermediate-depth earthquakes in the Japan and northern Chile subduction zones, which are considered representatives of cold and warm slabs, respectively, and for which decent initial catalogs exist owing to data from local/regional seismic deployments. Finally, we analyze the result in terms of the width of double seismic zones and the relationship between depth phases differential times and discuss the effect of dehydration.

## 2 Data and Methods

### 2.1 Data selection and processing

We use the vertical component of broad-band waveform data from earthquakes at teleseismic distances (from 30 to 95 degrees). Event epicenters and depths obtained from regional or global catalogs, such as NEIC-USGS, ISC, or ISC-EHB [Engdahl *et al.*, 1998], are used as initial estimates for calculating travel time and then determining time windows consisting phases of interest. We cut the teleseismic waveform using 10 s before and 100 s after the time of the P-wave arrival calculated from the *ak135* global wave speed model [Kennett *et al.*, 1995], which is sufficient to include depth phases of intermediate-depth earthquakes. The waveforms thus selected are resampled to 10 Hz and tapered on both sides. We then filter them using a second-order Butterworth band-pass filter with low and high cut-off frequencies of 0.2 and 2 Hz, respectively. Removing instrument responses is not necessary as their spectral amplitude is flat in this frequency range. Finally, we auto-correlate the waveforms after spectral broadening [Pham and Tkalčić, 2017, Eq. (2)] using a frequency window length of 1.0 Hz. The spectral broadening is an important step in our data processing since it balances the frequency components so that the resultant auto-correlograms are not dominated by low frequency components. This is similar to running-absolute-mean normalization [Bensen *et al.*, 2007] in order to suppress the effects of large seismic events in the time domain.

Since the arrival time of depth phases associated with intermediate earthquakes changes slowly and is much less sensitive to epicentral distance than to focal depth, we apply a simple move-out correction to a reference epicentral distance. The correction time is calculated based on the initial location and the global 1D velocity model *ak135* [Kennett *et al.*, 1995]. We then stack all the individual auto-correlograms linearly to obtain the final auto-correlogram at the reference epicentral distance. In cases where station distribution is relatively sparse a phase weighted stack [Rost, 2002] can help to increase the signal to noise ratio. The envelope, that is, the energy associated with depth phases is used to project back to the depth using a 3D velocity model, if available, or *ak135*.

### 2.2 Validation with a $M_w 4.5$ intermediate-depth earthquake in northern Chile

We illustrate and validate our method using an intermediate-depth earthquake in northern Chile (moment magnitude  $M_w 4.5$ , focal depth 111.3 km according to the NEIC-

USGS catalog) and recordings from 1948 broadband seismic stations at teleseismic distances (Fig. 1a). For this relatively small earthquake, the first arrivals are not clear at teleseismic distances (Fig. 1b), making techniques based on first arrival identification challenging [e.g. *Craig*, 2019; *Bonner et al.*, 2002]. In contrast, our method based on P wave auto-correlation (with move-out correction using the initial depth of 111.3 km to a reference distance of 70°) shows clearly the arrival of energy associated with the pP and sP phases, although sP phase is weaker than pP (more about this later). The first 60 s of 400 randomly selected auto-correlograms (Fig. 1c) reveals pP signal around 26.4 s, which becomes clearer after stacking. The pP arrival time (along with ak135) allows the refinement of the focal depth from 111.3 km according to the NEIC-USGS catalog to 105.3 km.

Using auto-correlation to extract depth phase energy is not new and has been applied elsewhere for depth relocation with data from stations at both local and teleseismic distances [e.g. *Audet and Ma*, 2018; *Tibuleac*, 2014; *Zhang et al.*, 2014]. One of the main differences with our method is that we apply spectral broadening to increase the high-frequency content and facilitate depth phases detection. In fact, the stacking of auto-correlograms without spectral broadening does not show a clear depth phase signal either with linear or phase weighted stacking (Fig. 2a). The spectrum of the auto-correlograms is squared after auto-correlation, which will cause the auto-correlograms dominated by even lower frequencies if the original (band-limited) signal has strong low-frequency components, as is usually the case for teleseismic data because of the attenuation of high-frequency components compared to that of low frequencies. The ‘spectral whitening’ that we use also turns out to be important in applications of retrieving near station reflections [*Oren and Nowack*, 2016; *Pham and Tkalčić*, 2017, 2018].

We found our results do not critically depend on the actual depth used for move-out correction, as long as the correction depth is within 20 km of the true depth. We verified this by varying the move-out correction depth from 83 to 133 km and found all of them show coherent stacking, which leads to clear pP and sP energy – the sP phase is weaker for this event but still stands out with a larger amplitude than the noise (Fig. 2b). This is not surprising since the difference in correction time between different depths is quite small. For this particular example, the correction time at 30 degrees is less than 1 second for correction depths of 85 and 105 km (Fig. 2c). Moreover, most stations are located between 50 to 80 degrees, which further reduces the sensitivity to the actual depth used for move-out correction.

Structural heterogeneity in the mantle and topography near the depth phase reflections at the surface may degrade the coherency of the stack using the global array. However, we found the stacks are usually dominated by the most densely distributed stations. Indeed, for this earthquake, stacking data only from the stations in the US also show a clear pP signal (Fig. S1a). To assess the influence of bounce-point topography, we grouped stations in the US in eastern and western part based on the back azimuth of station and event pairs. The results still show coherent stacking. The pP arrival using stations in the eastern US shows a slightly delayed phase due to the high elevation of Andes, but this only has a minor effect since the envelope is used to determine the depth (Fig. S1b).

A more straightforward way would be to stack the auto-correlograms along a depth phase arrival time curve predicted from a 3D wavespeed model and use the depth that yields the maximum stack value. This is equivalent to stacking with move-out correlation based on the true depth. We found, however, that the effect on depth estimation is negligible if the initial depth is within 20 km of the true depth (Fig. 2b), which is a reasonable tolerance given the uncertainty in focal depth estimates in global catalogs. For the test event used here, the focal depth from direct stacking based on a phase arrival time curve is 105.0 km (Fig. S2), which is very close to the result (105.3 km) obtained from stacking after move-out correction.

### 3 Applications to Japan and northern Chile subduction zones

Japan and northern Chile subduction zones are representative end members of cold (old tectonic plate) and warm (young) subduction, respectively [Müller *et al.*, 1997]. Intermediate-depth earthquakes in these regions are routinely located with local seismic data [e.g. Kita *et al.*, 2006; Sippl *et al.*, 2018]. To refine the depth locations of earthquakes in these regions so that one can understand the mechanisms of intermediate-depth earthquakes better, we apply our method to extract the depth phase energy using the ISC catalog for Japan and a local catalog from Sippl *et al.* [2018] in northern Chile. We assume that the epicenter locations are relatively well constrained and use the additional constraints from depth phases only to improve estimates of focal depths.

From 2004 to 2018, for this region (139.0E-143.0E, 38.5N-40.5N) the ISC catalog includes 184 earthquakes with moment magnitude larger than 4.0 and focal depths ranging from 50 to 300 km. We applied our method to these earthquakes and manually



checked all the stacked auto-correlograms. We successfully extracted 65 events with signal to noise ratio around the stacked pP or sP larger than 10.0. The smallest magnitude that still yielded acceptable stacks is  $M_w 4.0$  (Fig. S3). For the range of focal depths considered, the depth phases (pP and sP) are well separated in time. We apply a double-difference relocation algorithm [Waldhauser and Ellsworth, 2000; Florez and Prieto, 2017] to our pP and sP data in order to decrease the effect of 3D wavespeed variation in the subduction zones. Unfortunately, the sparse source distribution only allows us to relocate a small fraction of events (Fig. S4). Therefore, we also incorporate direct relocation by taking the average of depths determined by sP and pP if both are available. Otherwise, we determine the phase type based on the predicted arrival time range using a depth window of 40 km around the initial depth and then relocate accordingly in cases where we only have one clear depth phase (pP or sP). Although it relies heavily on the initial depths, we found little ambiguity in deciding the phase types (pP or sP), thanks to the good initial catalogs. We combine direct and double-difference relocation and take the average depth as our final depth, given that the difference between them is small (Fig. S4). The relocation reveals a well-defined double seismic zone (Fig. 3a), with a width of about 30 km between the upper and the lower layer, which is consistent with *Brudzinski et al.* [2007] and *Florez and Prieto* [2019].

In northern Chile, we extract all earthquakes from the catalog of *Sippl et al.* [2018] in our study region (70.5W-68.5W, 23.0S-21.0S) from 2007 to 2015, with magnitudes larger than 4.0 and depths from 40 to 100 km. This results in 227 earthquakes and we successfully relocated 84 of them, with 4.1 the smallest magnitude that still yields a useful stack (Fig. S3). We note that the detectability does not correlate with event magnitude, both for Japan and northern Chile (Fig. S3). Sometimes earthquakes with similar magnitudes and nearly the same station distribution show different stacking results (Fig. S5), which may indicate the effects of earthquake focal mechanism due to heterogeneous stress distribution [Chang et al., 2017]. Similar to the relocated events in the Japan subduction zone, the refined event depths also delineate a double seismic zone (Fig. 3b), with a width of about 14 km between two layers, consistent with *Rietbrock and Waldhauser* [2004].

We compare our relocations with existing catalogs from Japan Meteorological Agency (JMA) and ISC-EHB [Engdahl et al., 1998] in Japan, and ISC-EHB as well as catalogs from *Sippl et al.* [2018] and *Craig* [2019] in northern Chile. We found the new relocated events delineate the double seismic zones better, with less scattered events along different

interfaces. It is not entirely surprising that our method using teleseismic depth phases improves the depth locations in the catalog that are derived from local seismic data, considering relocations based on first arrival times suffer from the trade-off between earthquake origin time and depth.

Water and high pore pressure can increase the  $V_p/V_s$  dramatically in the source region [e.g. *Kodaira et al.*, 2004; *Audet et al.*, 2009; *Peacock et al.*, 2011]. To characterize the dehydration effect in the subduction zones better, we pick the differential arrival times ( $\Delta t_{pP} = t_{pP} - t_P$  and  $\Delta t_{sP} = t_{sP} - t_P$ ) from stacked auto-correlograms with both clear pP and sP energy and then calculate  $(\Delta t_{sP}^{obs} - \Delta t_{pP}^{obs}) - (\Delta t_{sP}^{syn} - \Delta t_{pP}^{syn})$ , that is, the observed differential time between sP and pP, and compared them with the ones predicted from the global 1D ak135 model [*Kennett et al.*, 1995]. The results are shown in Fig. 4. For both the Japan and northern Chile subduction zone, we found most earthquakes with positive values, that is, advanced pP and thus larger  $V_p/V_s$ , are located in the upper layer of the double seismic zones inside the oceanic subducting slab. These earthquakes are mostly limited to above 80 km in Japan but continue deeper (to about 100 km) in the upper layer of the north Chilean slab. However, due to the large uncertainty in the slab interface [*Hayes et al.*, 2018] and depth locations based on the 1D wavespeed model, it is uncertain if these earthquakes are in the subducting oceanic crust or mantle. For the lower layer, we did not observe anomalous positive values in either subduction zones, indicating small  $V_p/V_s$  and thus, a dry lower layer.

The differential time between sP and pP is sensitive to the average  $V_p/V_s$  between the event and the surface. In order to estimate  $V_p/V_s$ , we adopt an idea from double-difference relocation and take two events, one in the lower layer and the other in the upper layer. We then calculate the differential time relative to one another, which is most sensitive to the  $V_p/V_s$  between the upper and the lower layer (Fig. S6). The obtained relative differential time between two events is smaller than the one calculated from ak135, indicating, again, decreased  $V_p/V_s$  between the two layers in the double seismic zone.

## 4 Discussion and Conclusions

In this paper, we investigated the possibility of using P-wave auto-correlation to detect energy associated with arrivals of the depth phases pP and sP to improve focal depth estimates of intermediate-depth earthquakes and characterize the  $V_p/V_s$  ratio around the

source regions. The method relies on the small sensitivity of depth phase arrival time with respect to epicentral distance, which allows stacking of data from all stations at a teleseismic distance to improve the signal-to-noise ratio of the phases of interest. Picking arrivals is not needed and since the method can be applied to earthquakes with magnitude as small as the  $M_w 4.0$ , our analysis can benefit from more events than traditional studies. This also indicates the potential for wider application. For example, the application to the global intermediate to deep earthquake catalog could improve depth estimation of more small-magnitude earthquakes, which could help improve seismic imaging and tomography as well as the understanding of the mechanisms of those enigmatic earthquakes.

We applied this method to improve the depth of the intermediate earthquakes in two end members of subduction zones, the young/warm northern Chile subduction zone and the old/cold Japan subduction zone. Our results provide further evidence of the positive correlation between the slab ages and the width of double seismic zones, confirming that temperature plays a key role in controlling the geometry of double seismic zones. We note that this observation does not necessarily imply that dehydration embrittlement controls intermediate-depth earthquakes since the preferred condition of temperature ( $600 - 800^\circ\text{C}$ ) in thermal shear instability mechanism also predicts narrow widths of double seismic zones in warm slabs.

Recently findings of correlation of seismicity rate and off-trench faults distribution [Boneh *et al.*, 2019], deep hydration in the Mariana subduction zone [Cai *et al.*, 2018], and high  $V_p/V_s$  in the lower layer in northern Chile [Bloch *et al.*, 2018], point to a dehydration embrittlement mechanism for intermediate earthquakes. However, the high  $b$  value in the upper layer [Florez and Prieto, 2019] may lead to the dominance of upper layer seismicity in estimating the seismicity rate in the intermediate depth range, thus suppressing the contribution of lower layer seismicity which may operate with other mechanisms. Hydration to about 24 km below the Moho in the Mariana subduction zone, as observed by Cai *et al.* [2018], may not be deep enough to reach the lower layer in the double seismic zone, whose width may reach 40 km [Brudzinski *et al.*, 2007; Florez and Prieto, 2019]. Neither in Japan nor Chile do we find anomalous  $sP$  to  $pP$  differential times for events in the lower layers of the double seismic zones, which argues against deep penetration of water into the upper mantle and, thus, dehydration embrittlement as the mechanism for the lower of the double seismic zone. This is somewhat inconsistent with Bloch *et al.* [2018], who observed very high  $V_p/V_s$  in the lower layer. But the depth where they found anoma-

lous  $V_p/V_s$  (about 55 km) is shallower than what we observed with sP to pP differential time. Using a similar approach to *Lin and Shearer* [2007] and *Bloch et al.* [2018], we do not find high  $V_p/V_s$  in the lower layer in the Japan subduction zone (Fig. S7). It could be interesting to explore deeper regions in the lower layer of the double seismic zone in northern Chile using the approach of *Bloch et al.* [2018] to see if both measurements are consistent with each other and confirm if dehydration extends deeper in the lower layer in warm slabs.

The events that are above 80 km and 60 km in the Japan and northern Chile subduction zones, respectively, seem located mostly in the oceanic crust according to global or regional slab models [*Hayes et al.*, 2018; *Kita et al.*, 2010] and may result from dehydration. This would be consistent with some observations, such as water infiltration in the trench outer rise [*Ranero et al.*, 2003], positive correlation of seismicity rate and fault density [*Boneh et al.*, 2019], and low velocity in the crust using guided waves [*Shiina et al.*, 2017]. Along with the low  $V_p/V_s$  in the lower layer in the double seismic zones, this may indicate that two mechanisms operate on the intermediate-depth earthquakes [*Florez and Prieto*, 2019]. In view of uncertainty in both slab interfaces and event locations this needs further study.

The negative to normal to differential times in the lower layer indicates that earthquakes in the lower layer are not associated with anomalous high  $V_p/V_s$  or dehydration. Combined with recent experimental results that suggest that thermal runaway could occur in both hydrous and anhydrous minerals [*Ohuchi et al.*, 2017], our results are consistent with thermal instability for generating intermediate earthquakes, or stress transfer which requires little dehydration [*Ferrand et al.*, 2017; *Scambelluri et al.*, 2017], and argue against dehydration embrittlement as the primary mechanism, at least not in the lower layer of double seismic zones.

## Acknowledgments

Comments and advice from the Editor (Gavin Hayes) and the two anonymous reviewers greatly helped us improve our manuscript. We acknowledge the fruitful discussion with Thanh-Son Pham, which inspired us to extend the auto-correlation technique to extract depth phases. We thank Aurélien Mordret, Nori Nakata, Rachel E. Abercrombie, and Victor Tsai for many insightful discussions. Malcolm White's comments on the early version of the manuscript are also appreciated. Most of the figures are generated using GMT

[Wessel *et al.*, 2013]. Obspy [Beyreuther *et al.*, 2010] is used for some of the data processing. Raw seismic waveforms were downloaded from the IRIS DMC (<http://ds.iris.edu/ds/nodes/dmc/data/>). Catalogs containing initial locations in northern Chile and Japan were obtained from Sippl *et al.* [2018] and ISC (<http://www.isc.ac.uk/iscbulletin/>). The relocated catalog is provided in the supporting information.

## References

- Audet, P., and S. Ma (2018), Deep crustal earthquakes in the Beaufort sea, western Canadian arctic, from teleseismic depth phase analysis, *Seismological Research Letters*, 89(4), 1379–1384, doi:10.1785/0220180047.
- Audet, P., M. G. Bostock, N. I. Christensen, and S. M. Peacock (2009), Seismic evidence for overpressured subducted oceanic crust and megathrust fault sealing, *Nature*, 457(7225), 76.
- Bensen, G. D., M. H. Ritzwoller, M. P. Barmin, A. L. Levshin, F. Lin, M. P. Moschetti, N. M. Shapiro, and Y. Yang (2007), Processing seismic ambient noise data to obtain reliable broad-band surface wave dispersion measurements, *Geophysical Journal International*, 169(3), 1239–1260, doi:10.1111/j.1365-246x.2007.03374.x.
- Beyreuther, M., R. Barsch, L. Krischer, T. Megies, Y. Behr, and J. Wassermann (2010), Obspy: A python toolbox for seismology, *Seismological Research Letters*, 81(3), 530–533.
- Bloch, W., T. John, J. Kummerow, P. Salazar, O. S. Krüger, and S. A. Shapiro (2018), Watching dehydration: Seismic indication for transient fluid pathways in the oceanic mantle of the subducting nazca slab, *Geochemistry, Geophysics, Geosystems*, 19(9), 3189–3207.
- Boneh, Y., E. Schottenfels, K. Kwong, I. Zelst, X. Tong, M. Eimer, M. S. Miller, L. Moresi, J. M. Warren, D. A. Wiens, M. Billen, J. Naliboff, and Z. Zhan (2019), Intermediate-depth earthquakes controlled by incoming plate hydration along bending-related faults, *Geophysical Research Letters*, 46(7), 3688–3697, doi: 10.1029/2018gl081585.
- Bonner, J. L., D. T. Reiter, and R. H. Shumway (2002), Application of a cepstral f statistic for improved depth estimation, *Bulletin of the seismological Society of America*, 92(5), 1675–1693.

- Brudzinski, M. R., C. H. Thurber, B. R. Hacker, and E. R. Engdahl (2007), Global prevalence of double benioff zones, *Science*, *316*(5830), 1472–1474.
- Cai, C., D. A. Wiens, W. Shen, and M. Eimer (2018), Water input into the mariana subduction zone estimated from ocean-bottom seismic data, *Nature*, *563*(7731), 389.
- Chang, Y., L. M. Warren, and G. A. Prieto (2017), Precise locations for intermediate-depth earthquakes in the cauca cluster, colombia, *Bulletin of the Seismological Society of America*, *107*(6), 2649–2663.
- Chen, M., V. C. Manea, F. Niu, S. S. Wei, and E. Kiser (2019), Genesis of intermediate-depth and deep intraslab earthquakes beneath Japan constrained by seismic tomography, seismicity, and thermal modeling, *Geophysical Research Letters*, *46*(4), 2025–2036, doi:10.1029/2018gl080025.
- Chernak, L. J., and G. Hirth (2011), Syndeformational antigorite dehydration produces stable fault slip, *Geology*, *39*(9), 847–850, doi:10.1130/g31919.1.
- Craig, T. J. (2019), Accurate depth determination for moderate-magnitude earthquakes using global teleseismic data, *Journal of Geophysical Research: Solid Earth*, *124*(2), 1759–1780, doi:10.1029/2018jb016902.
- Deseta, N., T. Andersen, and L. Ashwal (2014), A weakening mechanism for intermediate-depth seismicity? detailed petrographic and microtextural observations from blueschist facies pseudotachylytes, cape corse, corsica, *Tectonophysics*, *610*, 138–149.
- Dobson, D. P. (2002), Simulation of subduction zone seismicity by dehydration of serpentine, *Science*, *298*(5597), 1407–1410, doi:10.1126/science.1075390.
- Engdahl, E. R., R. van der Hilst, and R. Buland (1998), Global teleseismic earthquake relocation with improved travel times and procedures for depth determination, *Bulletin of the Seismological Society of America*, *88*(3), 722–743.
- Ferrand, T. P., N. Hilaret, S. Incel, D. Deldicque, L. Labrousse, J. Gasc, J. Renner, Y. Wang, H. W. G. II, and A. Schubnel (2017), Dehydration-driven stress transfer triggers intermediate-depth earthquakes, *Nature Communications*, *8*(1), doi:10.1038/ncomms15247.
- Florez, M. A., and G. A. Prieto (2017), Precise relative earthquake depth determination using array processing techniques, *Journal of Geophysical Research: Solid Earth*, *122*(6), 4559–4571, doi:10.1002/2017jb014132.

- Florez, M. A., and G. A. Prieto (2019), Controlling factors of seismicity and geometry in double seismic zones, *Geophysical Research Letters*, 46(8), 4174–4181, doi:10.1029/2018gl081168.
- Green, H. (1995), The mechanics of deep earthquakes, *Annual Review of Earth and Planetary Sciences*, 23(1), 169–213, doi:10.1146/annurev.earth.23.1.169.
- Grevemeyer, I., C. R. Ranero, E. R. Flueh, D. Kl<sup>í</sup>aschen, and J. Bialas (2007), Passive and active seismological study of bending-related faulting and mantle serpentinization at the Middle America trench, *Earth and Planetary Science Letters*, 258(3-4), 528–542, doi:10.1016/j.epsl.2007.04.013.
- Hacker, B. R., S. M. Peacock, G. A. Abers, and S. D. Holloway (2003), Subduction factory 2. are intermediate-depth earthquakes in subducting slabs linked to metamorphic dehydration reactions?, *Journal of Geophysical Research: Solid Earth*, 108(B1), doi:10.1029/2001jb001129.
- Hayes, G. P., G. L. Moore, D. E. Portner, M. Hearne, H. Flamme, M. Furtney, and G. M. Smoczyk (2018), Slab2, a comprehensive subduction zone geometry model, *Science*, 362(6410), 58–61.
- Houston, H. (2007), Deep earthquakes, in *Treatise on Geophysics*, pp. 321–350, Elsevier, doi:10.1016/b978-044452748-6.00071-7.
- John, T., S. Medvedev, L. H. R<sup>í</sup>upke, T. B. Andersen, Y. Y. Podladchikov, and H. Austrheim (2009), Generation of intermediate-depth earthquakes by self-localizing thermal runaway, *Nature Geoscience*, 2(2), 137–140, doi:10.1038/ngeo419.
- Jung, H., H. W. G. II, and L. F. Dobrzhinetskaya (2004), Intermediate-depth earthquake faulting by dehydration embrittlement with negative volume change, *Nature*, 428(6982), 545–549, doi:10.1038/nature02412.
- Jung, H., Y. Fei, P. G. Silver, and H. W. Green (2009), Frictional sliding in serpentine at very high pressure, *Earth and Planetary Science Letters*, 277(1-2), 273–279, doi:10.1016/j.epsl.2008.10.019.
- Kelemen, P. B., and G. Hirth (2007), A periodic shear-heating mechanism for intermediate-depth earthquakes in the mantle, *Nature*, 446(7137), 787–790, doi:10.1038/nature05717.
- Kemerait, R., and A. Sutton (1982), A multidimensional approach to seismic event depth estimation, *Geoexploration*, 20(1-2), 113–130.



- Kennett, B. L. N., E. R. Engdahl, and R. Buland (1995), Constraints on seismic velocities in the Earth from traveltimes, *Geophysical Journal International*, 122(1), 108–124, doi: 10.1111/j.1365-246x.1995.tb03540.x.
- Kita, S., T. Okada, J. Nakajima, T. Matsuzawa, and A. Hasegawa (2006), Existence of a seismic belt in the upper plane of the double seismic zone extending in the along-arc direction at depths of 70–100 km beneath NE Japan, *Geophysical Research Letters*, 33(24), doi:10.1029/2006gl028239.
- Kita, S., T. Okada, A. Hasegawa, J. Nakajima, and T. Matsuzawa (2010), Anomalous deepening of a seismic belt in the upper-plane of the double seismic zone in the Pacific slab beneath the Hokkaido corner: Possible evidence for thermal shielding caused by subducted forearc crust materials, *Earth and Planetary Science Letters*, 290(3–4), 415–426.
- Kodaira, S., T. Iidaka, A. Kato, J.-O. Park, T. Iwasaki, and Y. Kaneda (2004), High pore fluid pressure may cause silent slip in the Nankai trough, *Science*, 304(5675), 1295–1298.
- Lin, G., and P. Shearer (2007), Estimating local  $v_p/v_s$  ratios within similar earthquake clusters, *Bulletin of the Seismological Society of America*, 97(2), 379–388.
- Müller, R. D., W. R. Roest, J.-Y. Royer, L. M. Gahagan, and J. G. Sclater (1997), Digital isochrons of the world's ocean floor, *Journal of Geophysical Research: Solid Earth*, 102(B2), 3211–3214.
- Obata, M., and S.-i. Karato (1995), Ultramafic pseudotachylite from the Balmuccia peridotite, Ivrea-Verbano zone, northern Italy, *Tectonophysics*, 242(3–4), 313–328, doi: 10.1016/0040-1951(94)00228-2.
- Ohuchi, T., X. Lei, H. Ohfuji, Y. Higo, Y. Tange, T. Sakai, K. Fujino, and T. Irifune (2017), Intermediate-depth earthquakes linked to localized heating in dunite and harzburgite, *Nature Geoscience*, 10(10), 771–776, doi:10.1038/ngeo3011.
- Okazaki, K., and G. Hirth (2016), Dehydration of lawsonite could directly trigger earthquakes in subducting oceanic crust, *Nature*, 530(7588), 81–84, doi:10.1038/nature16501.
- Oren, C., and R. L. Nowack (2016), Seismic body-wave interferometry using noise autocorrelations for crustal structure, *Geophysical Journal International*, 208(1), 321–332, doi:10.1093/gji/ggw394.
- Peacock, S. M. (2001), Are the lower planes of double seismic zones caused by serpentine dehydration in subducting oceanic mantle?, *Geology*, 29(4), 299–302.



- Peacock, S. M., N. I. Christensen, M. G. Bostock, and P. Audet (2011), High pore pressures and porosity at 35 km depth in the cascadia subduction zone, *Geology*, *39*(5), 471–474.
- Phạm, T.-S., and H. Tkalčić (2017), On the feasibility and use of teleseismic P wave coda autocorrelation for mapping shallow seismic discontinuities, *Journal of Geophysical Research: Solid Earth*, *122*(5), 3776–3791, doi:10.1002/2017jb013975.
- Phạm, T.-S., and H. Tkalčić (2018), Antarctic ice properties revealed from teleseismic P wave coda autocorrelation, *Journal of Geophysical Research: Solid Earth*, *123*(9), 7896–7912, doi:10.1029/2018jb016115.
- Prieto, G. A., M. Florez, S. A. Barrett, G. C. Beroza, P. Pedraza, J. F. Blanco, and E. Poveda (2013), Seismic evidence for thermal runaway during intermediate-depth earthquake rupture, *Geophysical Research Letters*, *40*(23), 6064–6068, doi:10.1002/2013gl058109.
- Ranero, C. R., J. P. Morgan, K. McIntosh, and C. Reichert (2003), Bending-related faulting and mantle serpentinization at the Middle America trench, *Nature*, *425*(6956), 367–373, doi:10.1038/nature01961.
- Ranero, C. R., A. Villaseñor, J. P. Morgan, and W. Weinrebe (2005), Relationship between bend-faulting at trenches and intermediate-depth seismicity, *Geochemistry, Geophysics, Geosystems*, *6*(12), n/a–n/a, doi:10.1029/2005gc000997.
- Reynard, B., J. Nakajima, and H. Kawakatsu (2010), Earthquakes and plastic deformation of anhydrous slab mantle in double Wadati-Benioff zones, *Geophysical Research Letters*, *37*(24), n/a–n/a, doi:10.1029/2010gl045494.
- Rietbrock, A., and F. Waldhauser (2004), A narrowly spaced double-seismic zone in the subducting Nazca plate, *Geophysical Research Letters*, *31*(10), doi:10.1029/2004gl019610.
- Rost, S. (2002), Array seismology: Methods and applications, *Reviews of Geophysics*, *40*(3), doi:10.1029/2000rg000100.
- Scambelluri, M., G. Pennacchioni, M. Gilio, M. Bestmann, O. Plümper, and F. Nestola (2017), Fossil intermediate-depth earthquakes in subducting slabs linked to differential stress release, *Nature Geoscience*, *10*(12), 960–966, doi:10.1038/s41561-017-0010-7.
- Shiina, T., J. Nakajima, and T. Matsuzawa (2013), Seismic evidence for high pore pressures in the oceanic crust: implications for fluid-related embrittlement, *Geophysical Research Letters*, *40*(10), 2006–2010.

- Shiina, T., J. Nakajima, T. Matsuzawa, G. Toyokuni, and S. Kita (2017), Depth variations in seismic velocity in the subducting crust: Evidence for fluid-related embrittlement for intermediate-depth earthquakes, *Geophysical research letters*, *44*(2), 810–817.
- Shillington, D. J., A. Bécel, M. R. Nedimović, H. Kuehn, S. C. Webb, G. A. Abers, K. M. Keranen, J. Li, M. Delescluse, and G. A. Mattei-Salicrup (2015), Link between plate fabric, hydration and subduction zone seismicity in Alaska, *Nature Geoscience*, *8*(12), 961–964, doi:10.1038/ngeo2586.
- Sippl, C., B. Schurr, G. Asch, and J. Kummerow (2018), Seismicity structure of the northern Chile forearc from >100,000 double-difference relocated hypocenters, *Journal of Geophysical Research: Solid Earth*, *123*(5), 4063–4087, doi:10.1002/2017jb015384.
- Tibuleac, I. M. (2014), A method for first-order earthquake depth estimation using super-arrays, *Seismological Research Letters*, *85*(6), 1255–1264, doi:10.1785/0220130212.
- Turner, H. H. (1922), On the arrival of earthquake waves at the antipodes, and on the measurement of the focal depth of an earthquake., *Geophysical Journal International*, *1*, 1–13, doi:10.1111/j.1365-246x.1922.tb05354.x.
- Ueda, T., M. Obata, G. D. Toro, K. Kanagawa, and K. Ozawa (2008), Mantle earthquakes frozen in mylonitized ultramafic pseudotachylytes of spinel-lherzolite facies, *Geology*, *36*(8), 607, doi:10.1130/g24739a.1.
- Vargas, J. A., N. M. Meqbel, O. Ritter, H. Brasse, U. Weckmann, G. Yáñez, and B. Godoy (2019), Fluid distribution in the central Andes subduction zone imaged with magnetotellurics, *Journal of Geophysical Research: Solid Earth*, *124*(4), 4017–4034, doi:10.1029/2018jb016933.
- Wadati, K. (1928), Shallow and deep earthquakes, *Geophys. Mag.*, *1*, 162–202.
- Waldhauser, F., and W. L. Ellsworth (2000), A double-difference earthquake location algorithm: Method and application to the northern hayward fault, california, *Bulletin of the Seismological Society of America*, *90*(6), 1353–1368.
- Wei, S. S., D. A. Wiens, P. E. van Keken, and C. Cai (2017), Slab temperature controls on the Tonga double seismic zone and slab mantle dehydration, *Science Advances*, *3*(1), e1601755, doi:10.1126/sciadv.1601755.
- Wessel, P., W. H. Smith, R. Scharroo, J. Luis, and F. Wobbe (2013), Generic mapping tools: improved version released, *Eos, Transactions American Geophysical Union*, *94*(45), 409–410.

525 Zhang, M., D. Tian, and L. Wen (2014), A new method for earthquake depth determi-  
526 nation: stacking multiple-station autocorrelograms, *Geophysical Journal International*,  
527 197(2), 1107–1116, doi:10.1093/gji/ggu044.

Author Manuscript

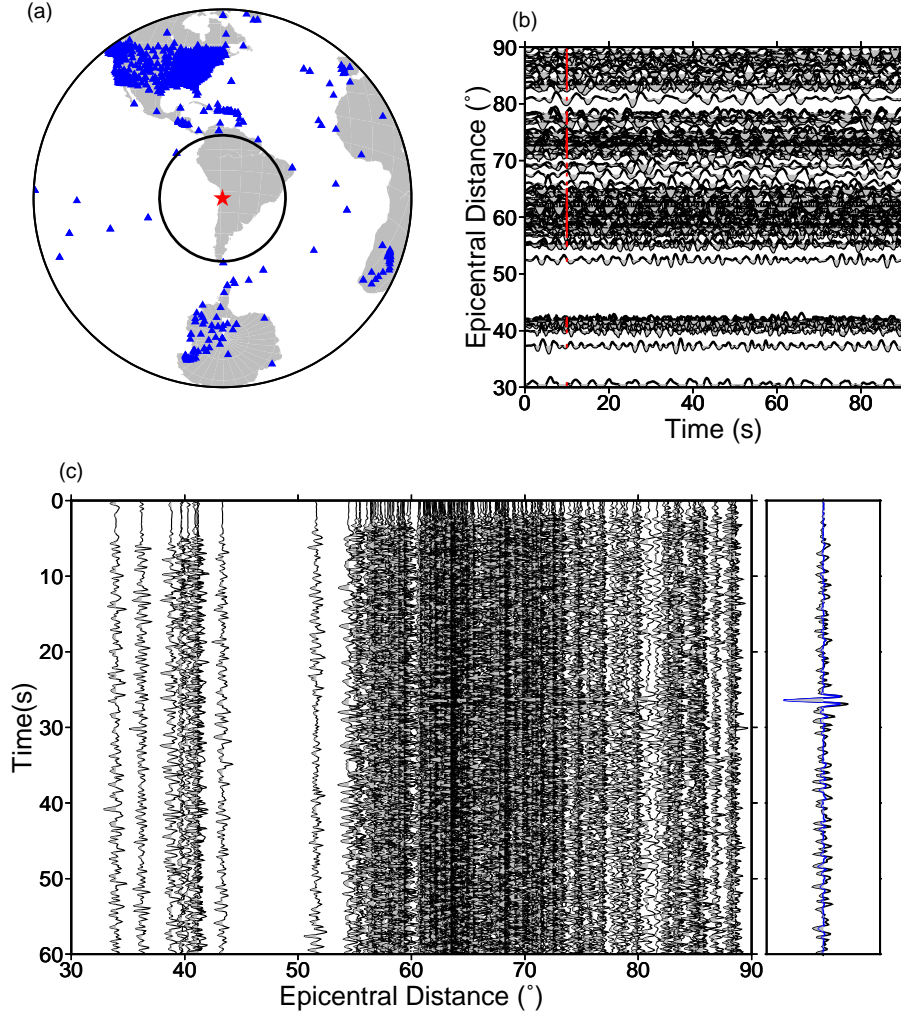


**Figure 1.** (a) The location of the April 11 2014 Mw4.5 northern Chile earthquake (red star) according to the NEIC-USGS catalog and the distribution of stations (blue triangles) used for extracting pP depth phase. (b) Raw waveforms after bandpass filtering from 0.2 to 2.0 Hz. Red bars mark the theoretical P wave arrival using the global ak135 model. (c) The individual auto-correlograms and linear stacking (black line) and phase weighted stacking records (blue line) after move-out correction. The large P signals at 0 second are tapered out.

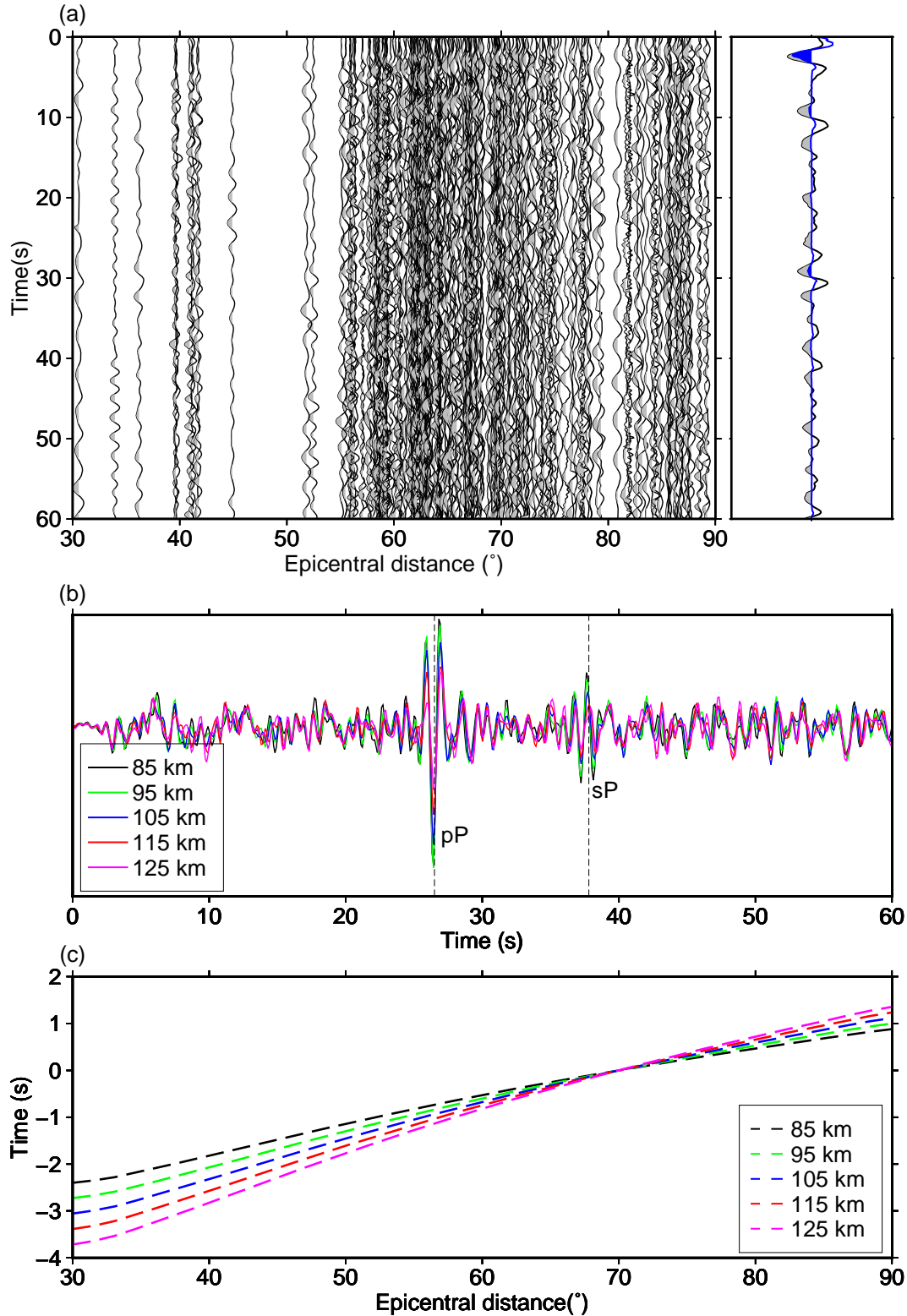


**Figure 2.** (a) Individual and stacked auto-correlograms for the April 11 2014 Mw4.5 northern Chile earthquake (Fig. 1a) after move-out correction but without spectral broadening. Black and blue line in the stack auto-correlograms represent linear and phase weighted stacking, respectively. (b) Stack auto-correlograms after move-out correction using different initial depths. (c) The move-out correction with respect to 70 degrees using different event depths at different epicentral distances.

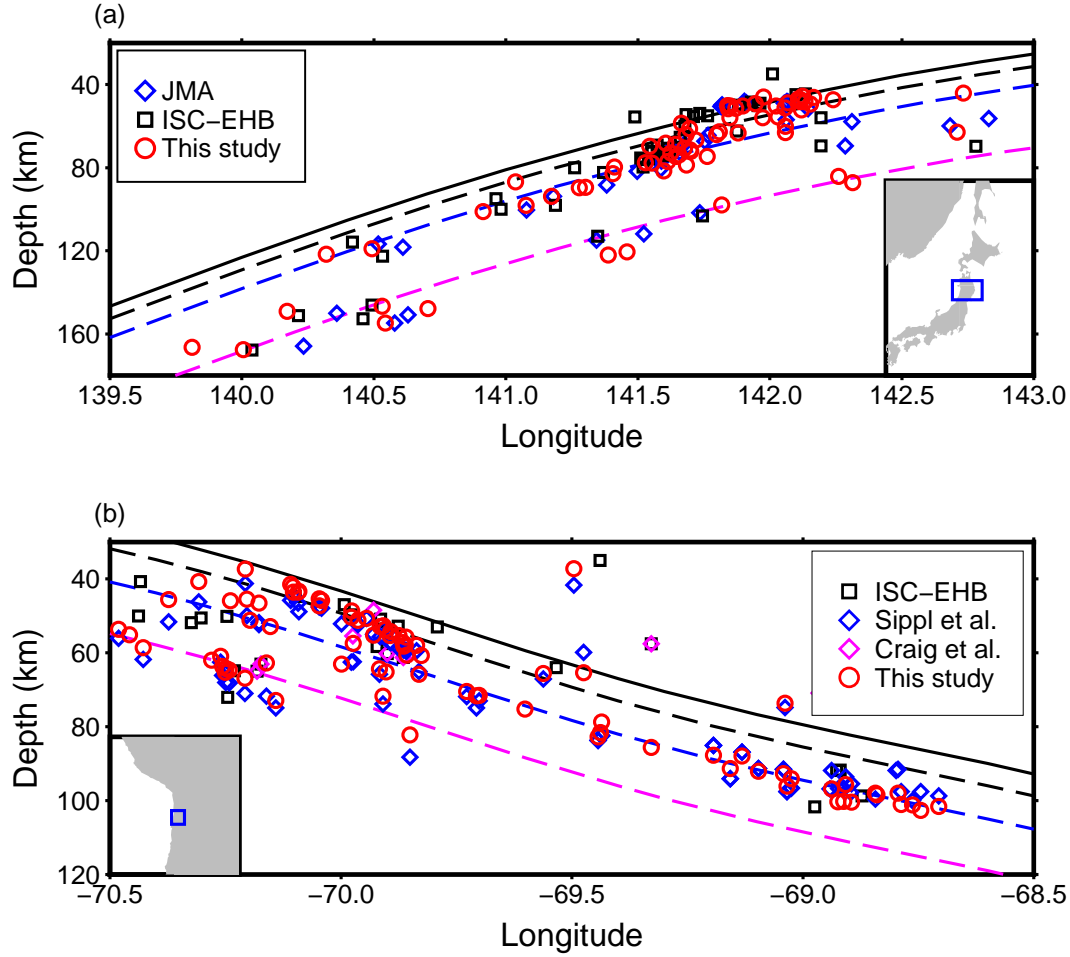


**Figure 3.** Relocated earthquakes in (a) Japan and (b) northern Chile subduction zones. Black squares show the locations from ISC-EHB catalog. Red circles show relocated earthquakes in this study. Blue diamonds show the locations from JMA and *Sippl et al.* [2018] in Japan and northern Chile subduction zones. Magenta diamonds show locations from *Craig* [2019]. Black solid lines show the slab interfaces from *Hayes et al.* [2018]. Black, blue and magenta dashed lines show oceanic Moho (6 km from the slab interface), the upper layer (15 km from the slab interface) and the lower layer (45 km and 29 km from the slab interface for the Japan and northern Chile subduction zones, respectively). Blue boxes in the inset figures show the study regions.

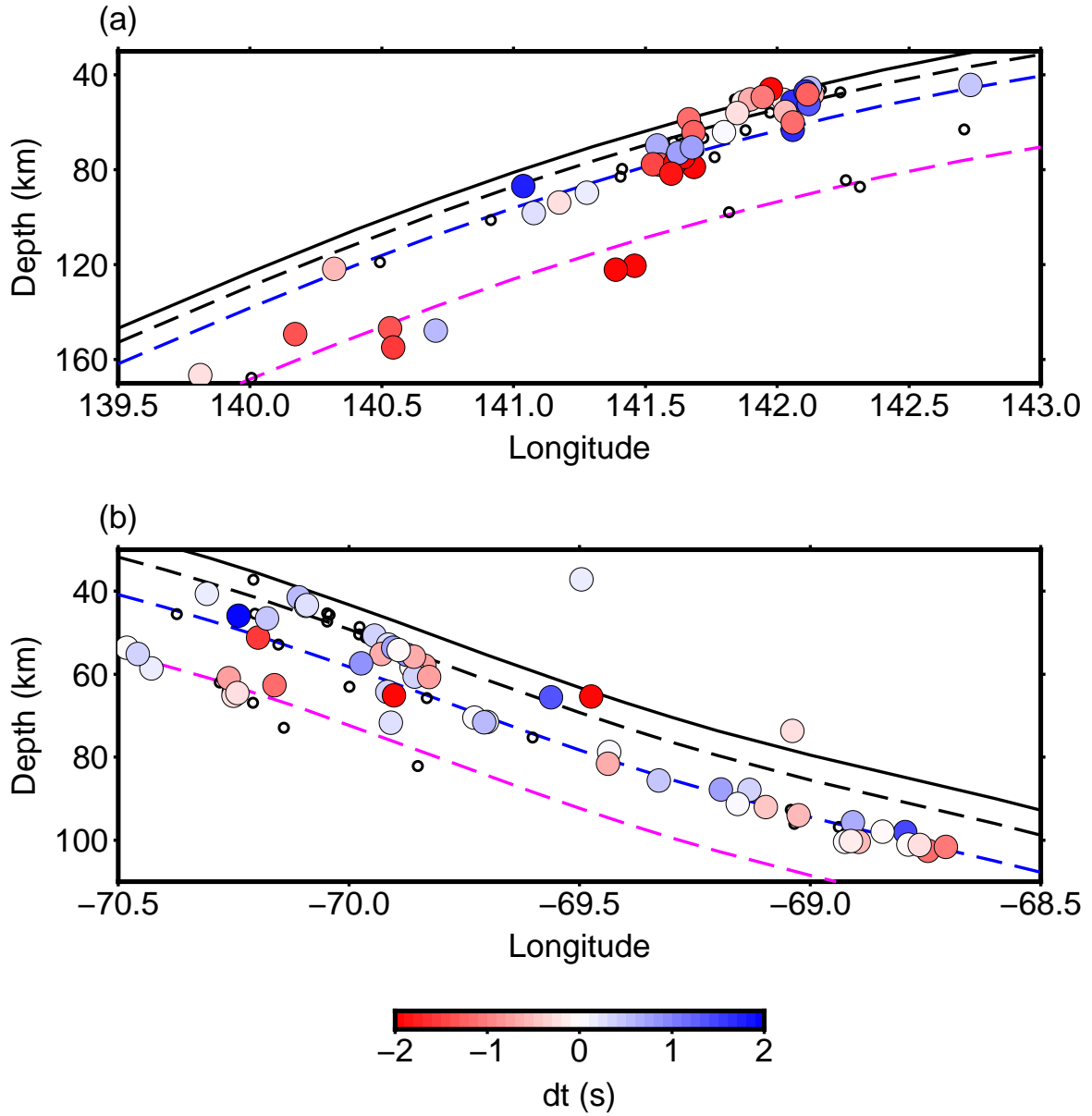


**Figure 4.** Residual of observed differential times between sP and pP and synthetic differential times using the global ak135 model in the Japan (a) and northern Chile (b) subduction zones. Negative values show advanced sP or delayed pP compared to that of ak135, indicating small average  $V_p/V_s$ . Small white circles show events only with either sP or pP. Solid and dashed lines are the same as Fig. 3.

Figure 1.

Author Manuscript



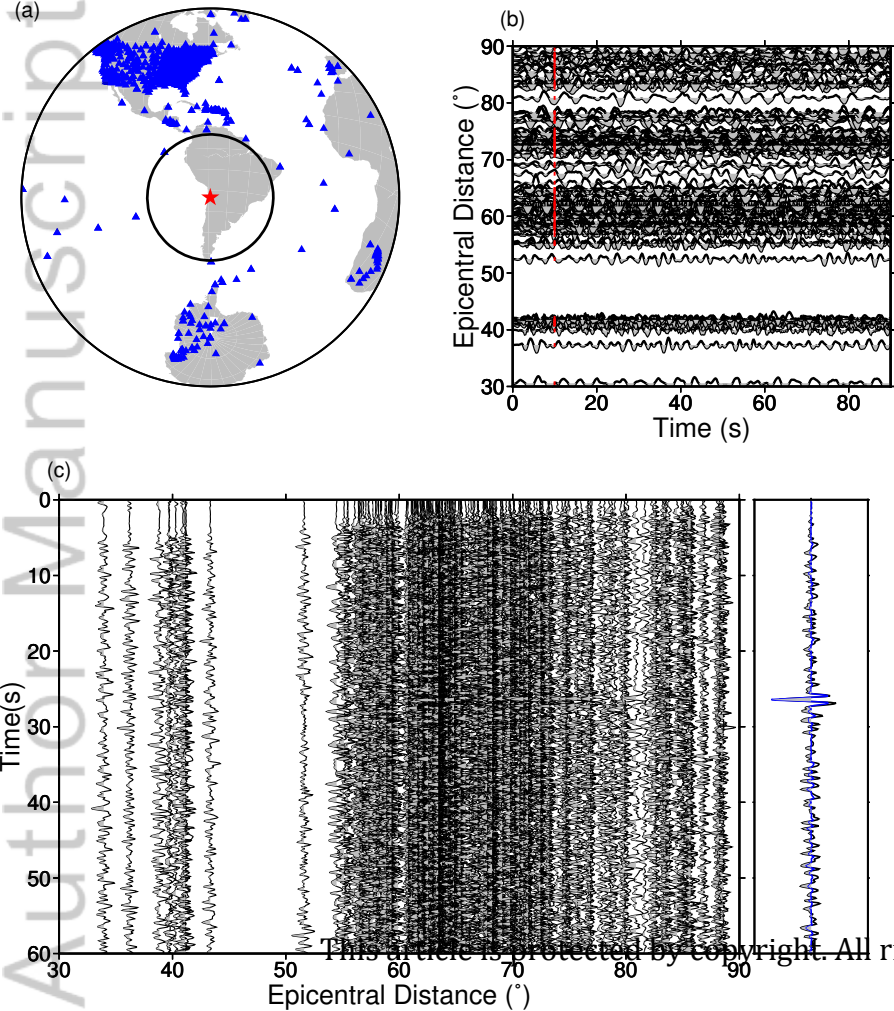


Figure 2.

Author Manuscript

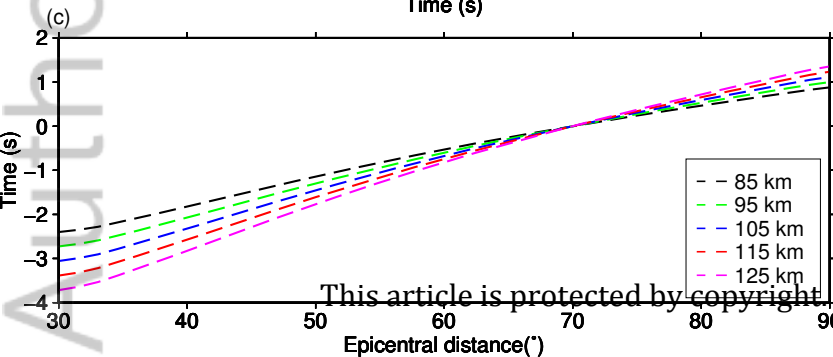
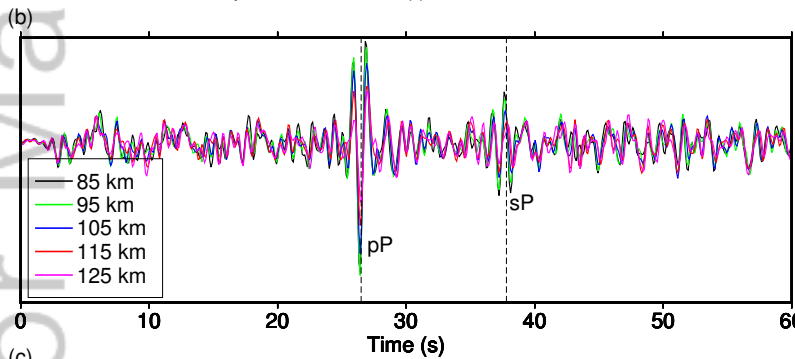
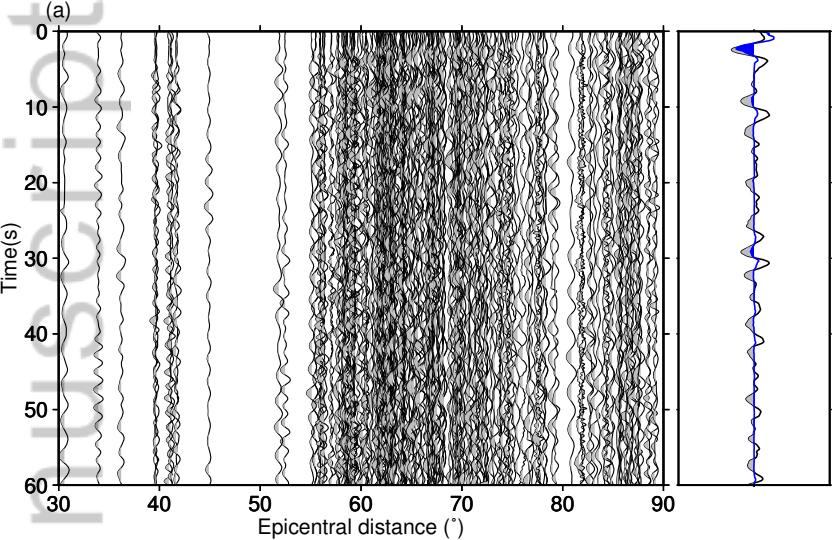


Figure 3.

Author Manuscript

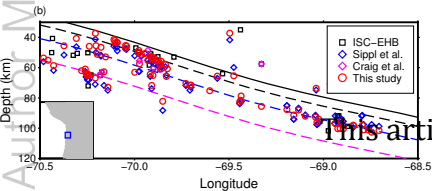
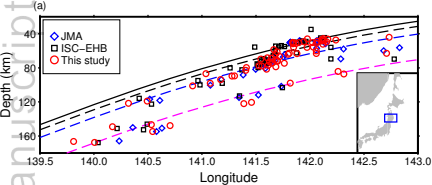
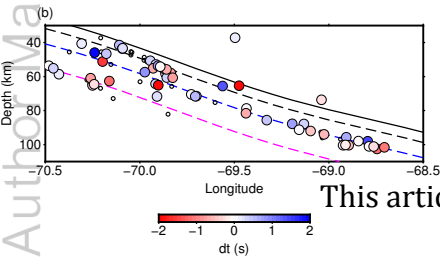
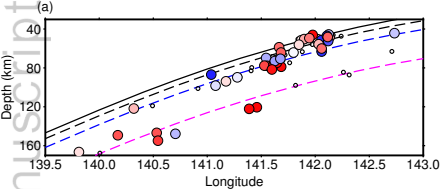
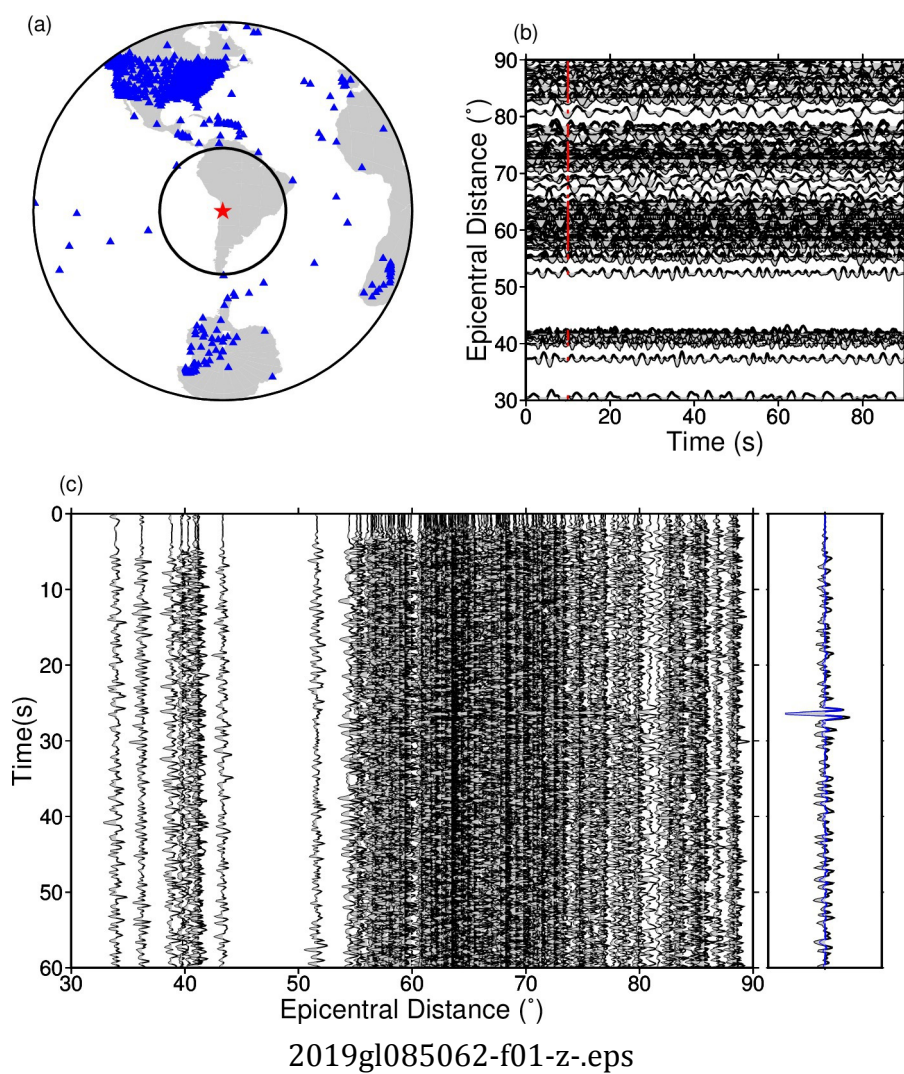


Figure 4.

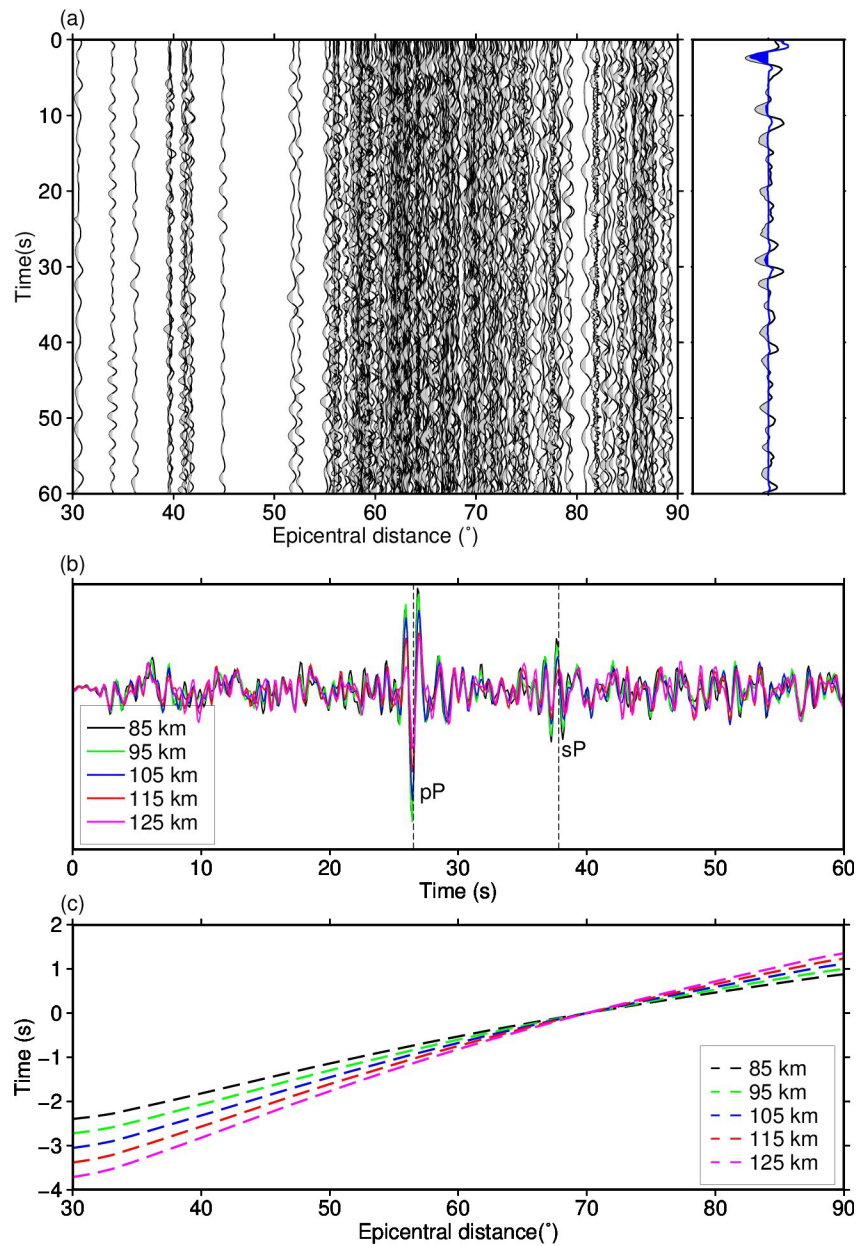
Author Manuscript



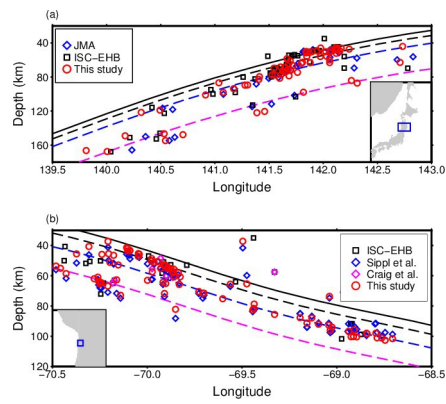


2019gl085062-f01-z-eps

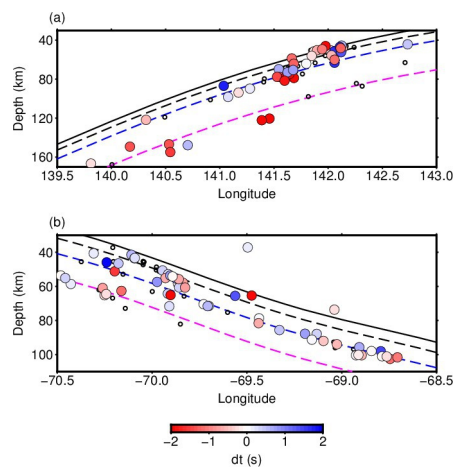




2019gl085062-f02-z-.eps



2019gl085062-f03-z-eps



2019gl085062-f04-z-eps